Exercise modulation of the host-tumor interaction in an orthotopic model of murine prostate cancer

Lee W. Jones,[1] Jodi Antonelli,[1] Elizabeth M. Masko,[1] Gloria Broadwater,[1] Christopher D. Lascola,[1] Diane Fels,[1] Mark W. Dewhirst,[1] Jason R. B. Dyck,[2] Jeevan Nagendran,[2] Catherine T. Flores,[1] Allison S. Betof,[1] Erik R. Nelson,[1] Michael Pollak,[3] Rajesh C. Dash,[1] Martin E. Young,[4] and Stephen J. Freedland[1,5]

[1]*Duke University Medical Center, Durham, North Carolina;* [2]*Cardiovascular Research Center and the Mazankowski Alberta Heart Institute, University of Alberta, Edmonton, Canada;* [3]*Department of Oncology and Lady Davis Research Institute, McGill University, Montreal, Canada;* [4]*University of Alabama at Birmingham, Birmingham, Alabama; and* [5]*Durham VA Medical Center, Durham, North Carolina*

Jones LW, Antonelli J, Masko EM, Broadwater G, Lascola CD, Fels D, Dewhirst MW, Nagendran JR, Flores CT, Betof AS, Nelson ER, Pollak M, Dash RC, Young ME, Freedland SJ. Exercise modulation of the host-tumor interaction in an orthotopic model of murine prostate cancer. *J Appl Physiol* 113: 263–272, 2012. First published May 17, 2012; doi:10.1152/japplphysiol.01575.2011.—The purpose of this study is to investigate the effects of exercise on cancer progression, metastasis, and underlying mechanisms in an orthotopic model of murine prostate cancer. C57BL/6 male mice (6–8 wk of age) were orthotopically injected with transgenic adenocarcinoma of mouse prostate C-1 cells (5×10^5) and randomly assigned to exercise ($n = 28$) or a non-intervention control ($n = 31$) groups. The exercise group was given voluntary access to a wheel 24 h/day for the duration of the study. Four mice per group were serially killed on *days 14*, *31*, and *36*; the remaining 38 mice (exercise, $n = 18$; control, $n = 20$) were killed on *day 53*. Before death, MRI was performed to assess tumor blood perfusion. Primary tumor growth rate was comparable between groups, but expression of prometastatic genes was significantly modulated in exercising animals with a shift toward reduced metastasis. Exercise was associated with increased activity of protein kinases within the MEK/MAPK and PI3K/mTOR signaling cascades with subsequent increased intratumoral protein levels of HIF-1α and VEGF. This was associated with improved tumor vascularization. Multiplex ELISAs revealed distinct reductions in plasma concentrations of several angiogenic cytokines in the exercise group, which was associated with increased expression of angiogenic and metabolic genes in the skeletal muscle. Exercise-induced stabilization of HIF-1α and subsequent upregulation of VEGF was associated with "productive" tumor vascularization with a shift toward suppressed metastasis in an orthotopic model of prostate cancer.

exercise; prostrate cancer

RANDOMIZED TRIALS DEMONSTRATE that structured endurance exercise is a safe and efficacious adjunct therapy to prevent and/or attenuate physiological as well as psychological adverse sequelae both during and following anticancer therapy in individuals diagnosed with cancer (12, 24). Given the beneficial effects of exercise on symptom control, a major research goal is to investigate whether exercise may also improve prognosis following a cancer diagnosis (13). Intriguingly, two recent observational studies report that regular exercise (≥3 h/wk, vigorous intensity exercise) is associated with a 61% and 57% reduction in the risk of cancer-specific mortality and progression following a diagnosis of early stage prostate cancer relative to inactive men (17, 23). The majority of prostate cancer deaths are due to metastatic disease, suggesting that exercise may inhibit tumor cell shedding (e.g., invasion, intravasation) from the primary tumor and/or propagation of tumor cells in distant ectopic sites (e.g., lungs, liver); confirmatory data from randomized trials are not currently available. Clearly, elucidation of the systemic and molecular mechanisms will be critical to inform hypothesis-driven clinical trials and ensure the optimal safety and efficacy of exercise in prostate cancer control.

Postulated mechanisms underlying the potential effects of exercise on cancer progression include modulation of circulating host levels of metabolic (e.g., markers of glucose-insulin homeostasis) and sex-steroid (e.g., testosterone) hormone levels, improvements in immune surveillance, and reduced systemic inflammation and oxidative damage (20). However, to date, there is a relative paucity of correlative or direct evidence on whether exercise modulates these host pathways or whether exercise-induced host modulation, in turn, influences the tumor phenotype (1). To this end, use of clinically relevant animal models provides an invaluable tool to understand at a systemic and molecular level how exercise modulates malignant progression and metastasis in vivo. To date, only two studies, to our knowledge, have examined the independent effects on exercise in a mouse model of prostate cancer. Specifically, Zheng et al. (30) found that exercise initiated 1 wk before tumor implantation (and continued for 63 days before implantation) significantly inhibited tumor growth as well as increased apoptosis in athymic mice bearing PC-3 subcutaneous human prostate xenografts. Similarly, Esser and colleagues (5) reported that 10 wk of voluntary running, particularly those animals running >5 km/day, delayed prostate cancer incidence/progression compared with those running <5 km/day in a C3(1)SV40Tag transgenic (spontaneous) model of prostate cancer.

However, the translational implications of these findings to the post-diagnosis prostate cancer clinical setting are not clear since exercise was initiated either before tumor inoculation (30) or immediately post-weaning (5) (i.e., prevention setting), and the Zheng et al. study utilized a suboptimal model (i.e., subcutaneous implantation of a human xenograft into immune deficient animals). Furthermore, the effects of exercise on circulating host-derived factors and other cardinal features of tumor progression (e.g., metastases, tumor perfusion, cell sig-

naling) were not evaluated. Against this background, we investigated the effects of exercise (after tumor establishment) on progression and metastasis by using an orthotopic model of murine prostate cancer. In addition, we also examined effects on the central features of the tumor phenotype including markers of metastatic potential, tumor blood perfusion/vascularization, hypoxia, angiogenesis, and cell signaling as well as changes in host-derived systemic inflammatory and metabolic growth factors. Finally, we also examined the effects on oxidative and metabolic gene expression in skeletal muscle hypothesized to modulate, in part, the exercise-systemic host relationship. We hypothesized that exercise would inhibit prostate cancer progression and metastasis.

MATERIALS AND METHODS

Mouse model and procedures. Seventy C57BL/6 male mice (6–8 wk of age; mean body weight, 26 ± 2 g) were obtained from Charles River (Wilmington, MA). All mice were individually housed (21°C with 35–45% humidity and a 12:12-h light-dark cycle) in cages with contact bedding and fed Purina Rodent Chow 5058 (LabDiet, Richmond, IN) and water ad libitum. Animal care was approved and in accordance with the Institutional Animal Care and Use Guidelines at Duke University Medical Center.

Transgenic adenocarcinoma of mouse prostate (TRAMP) C-1 cells were ordered through the Duke Cell Culture Facility from ATCC (Manassas, VA). TRAMP-C1 cell line was derived from the primary prostate tumor of a 32-wk-old TRAMP mouse and is tumorigenic in syngeneic C57/BL6 models. These cells are epithelial in nature and express the androgen receptor (6). Cells were cultured in DMEM supplemented with 5% FBS, 5% NuSerum IV (Collaborative Biomedical Products, Bedford, MA), 5 μg/ml insulin, and 10 nM dihydrotestosterone and harvested by trypsinization at ~80% confluence in log-phase growth. The study flow is presented in Fig. 1*A*. In brief, mice were allowed to acclimatize for 2 wk before experimental procedures. On *day −14*, all animals were injected orthotopically into the prostate with 0.1 ml of a 1:1 solution of TRAMP C-1 cells (5×10^5) and Matrigel (Becton Dickinson, Franklin Lakes, NJ) under general anesthesia with nembutol. Four mice died due to anesthesia/surgical complications, three died due to wound dehiscence, and four were excluded from further study due to a dermatologic condition of unknown diagnosis after veterinary examination. Fourteen days after implantation, the remaining 59 mice were randomly assigned to an exercise ($n = 28$) or a non-intervention control ($n = 31$) group.

The exercise modality in this experiment was voluntary wheel running as opposed to forced exercise paradigms (e.g., treadmill running). The selection of voluntary vs. forced exercise paradigms is based on a number of considerations, with advantages and disadvantages to each (7). Here, we selected voluntary wheel running since this exercise paradigm is more reflective of natural mouse locomotion/behavior (3a), whereas forced paradigms may induce a stress response (21a). Murine voluntary wheel running is characterized by intermittent exercise performed for relatively short time periods at high speed against a low load throughout the entire dark cycle (14). As such, voluntary wheel running reflects brief intermittent periods of physical activity that are consistent with the type of exercise behavior inversely correlated with mortality following a prostate cancer diagnosis (17, 23). However, the disadvantages of this modality are that exercise duration and intensity cannot be manipulated. Animals randomized to the exercise group were given voluntary access 24 h/day to a wheel measuring 11.5 cm in diameter, with wheel revolutions monitored continuously by magnetic sensor using the VitalView data acquisition program (Respironics, Murrysville, PA). Mice randomized to the control group were housed individually in identical cages but without wheels with contact bedding to control for environmental enrichment.

All mice were weighed, and running data were obtained twice weekly. Four mice per group were serially killed on *days 14*, *31*, and *36*; the remaining 38 mice (exercise, $n = 18$; control, $n = 20$) were killed on *day 53*. At necropsy (≥24 h after the last exercise bout), serum was obtained from cardiac puncture, whereas tumor (prostate gland and surrounding incorporated tissue), gross metastatic tissue (non-contiguous external masses that were grossly visible independent from the primary prostate tissue), and skeletal muscle (gastrocnemius) were surgically removed, weighed, and snap frozen at −80°C. Pathological confirmation of prostate cancer was performed on frozen tissue sections of 10-μm thickness stained with hematoxylin and eosin (H&E) and reviewed by a pathologist (R. C. Dash) blinded to group assignment.

Preparation of tissue lysate. A total of 1 ml of cell lysis buffer using the QProteome Mammalian Protein Preparation kit (Qiagen, Valencia, CA) was added to ~50 μg of primary prostate tumor tissue and was processed using a mechanical tissue homogenizer. Homogenates were centrifuged at 10,000 rpm for 20 min to clarify the lysates, and total protein concentration was determined using the BCA protein assay reagent (Thermo Fisher Scientific, Rockford, IL). All lysates were stored at −80°C until further analysis. All histological analysis was conducted only on samples obtained at the end of experimental procedures (*day 53*). Homogenized tumors from both groups were analyzed using commercially available ELISAs for content of VEGF and HIF-1 (Panomics, Fremont, CA; RayBiotech, Norcross, GA).

Immunohistochemistry. Frozen tissue sections were stained using specific antibodies. In brief, to stain for vasculature, sections were incubated for 1 h with rat anti-mouse CD31 antibody (BD Biosciences), diluted 1:100, followed by incubation with donkey anti-rat fluorescent secondary antibody (Alexa Fluor 488, Invitrogen), diluted 1:1,000. Pericyte coverage was assessed by α-smooth muscle actin (α-SMA) immunostaining. Following fixation and blocking, slides were treated with Cy3-conjugated mouse monoclonal anti-α-SMA (Sigma Aldrich), diluted 1:400, for 1 h. All antibodies were diluted in PBS and incubated at room temperature. All staining procedures ended with a 5-min application of Hoechst 33342 (Sigma Aldrich) to counterstain for cellular nuclei. Exclusion of the primary antibody served as a negative control. Slides were imaged using a high-resolution solid-state camera mounted on a fluorescent microscope (Axioscop Zplus, Carl Zeiss). All images were captured at ×5 magnification in 16-bit monochrome signal depth. Fixed exposure times were preselected for each fluorochrome. Image J (NIH) was used for all image analysis. The nuclear counterstain permitted region of interest contour lines to be drawn around each tumor and an optimal threshold were set for CD31 staining. The amount of positively stained area was divided by the total tumor area to obtain the area fraction of CD31. For the purpose of image presentation, pictures were taken using a Leica DMI6000CS inverted confocal microscope and Leica LAS AF 2.0 software.

Western blot analysis. Denatured samples of tissue homogenates were subjected to SDS-PAGE and subsequent immunoblotting to determine phosphorylation and expression of target proteins using the Fast Western Blot kit (Pierce-Thermo Scientific, Rockford, IL). Primary antibodies used for immunoblotting were anti-pAMPKα Thr^{172} (no. 2531), anti-pmTOR Ser^{2448} (no. 2971), anti-mTOR (no. 2972), and anti-pS6 kinase (no. 4858) from Cell Signaling Technology (Beverly, MA), anti-AMPKα2 (no. 19131) from Santa Cruz Biotechnology (Santa Cruz, CA), and anti-pAKT Ser^{473} (no. 05-669), anti-AKT (no. 05-591), and PI3 kinase (no. 06-195) from Millipore. Densitometric analysis was performed employing ImageJ software (NIH).

Membranes were blocked in 5% milk/Tris-buffered saline plus 0.1% Tween-20 (TBST) and then incubated with primary antibody in 1% milk/TBST overnight at 4°C. After being washed with TBST, the membranes were incubated with peroxidase-conjugated goat anti-rabbit or donkey anti-goat secondary antibody in 5% milk/TBST for

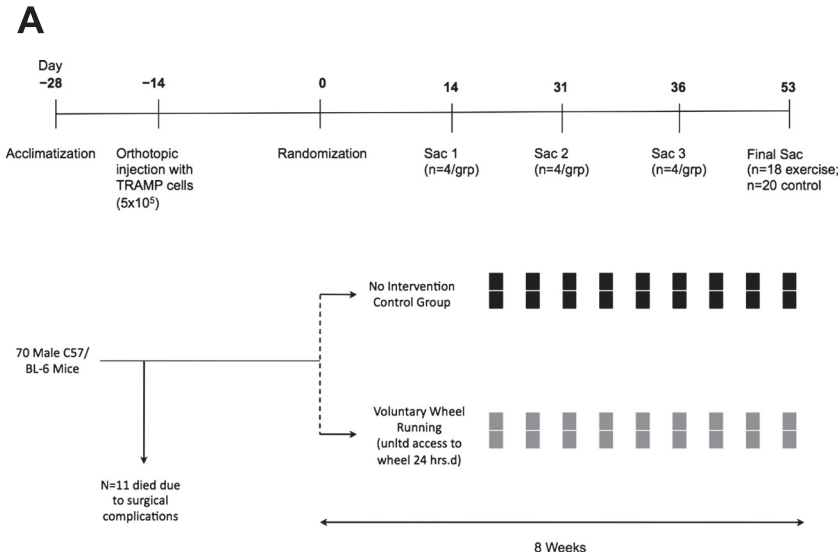

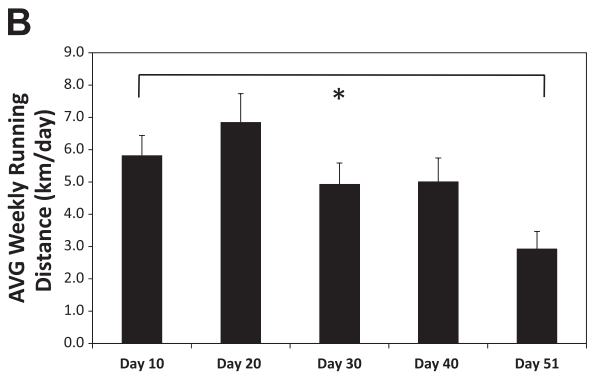

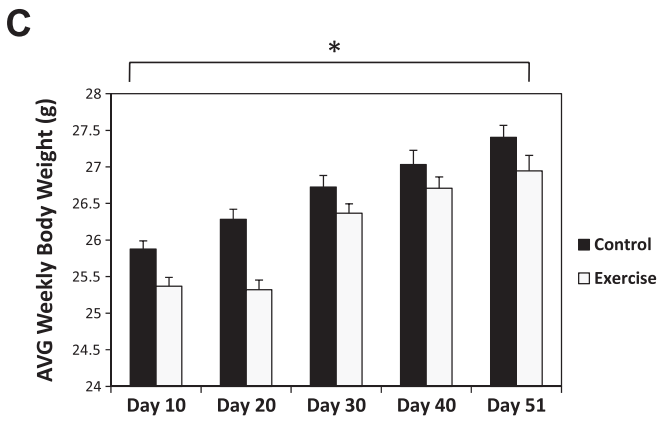

Fig. 1. *A*: study design/flow. *B*: voluntary wheel running distances every 10 days in C57/BL-6 male mice (n = 18–28/time point). Mean running distances with SE (error bars) are shown. Statistical significance was determined by a fixed-effects linear mixed model ($P < 0.001$). *C*: body weights over time of C57/BL-6 male mice randomized to voluntary wheel running or sedentary control (n = 18–28/group per time point). Mean body weights with SE (error bars) are shown. Statistical significance was determined by a fixed-effects linear mixed model ($P < 0.001$). All statistical tests were two-sided.

1.5 h at ambient temperature. After being washed further, the immune complexes were visualized with enhanced chemiluminescence reagent (Perkin Elmer). Densitometric analysis was performed employing ImageJ software (NIH).

Tumor and skeletal muscle gene profiling. Quantitative real-time PCR (QPCR) was performed as previously described (2). Tumors or muscle were pulverized under liquid N_2, and total RNA was harvested using the TRIzol method (Invitrogen, Carlsbad, CA), reverse transcribed (Bio-Rad), and amplified with iQ SYBRGreen Supermix (Bio-Rad). The relative quantitation method ($2^{-\Delta\Delta Ct}$) was used where all values were normalized to the TATA binding protein housekeeping gene. Data is presented with respect to non-intervention control. The purpose of skeletal muscle gene profiling is *1*) to confirm that exercise-induced muscle adaptations were sustained and *2*) given that local adaptations in the skeletal muscle activate release of cytokines into the peripheral circulation and that these cytokines may, in turn, influence tumor biology (10), to evaluate whether these genes were upregulated in response to exercise in the present model.

Magnetic resonance tumor blood perfusion imaging. Magnetic resonance (MR) imaging was performed on a Bruker 7T (70/30) system (Bruker Biospin, Billerica, MA) utilizing a quadrature surface receive and volume transmit coil setup with active decoupling. Animals were anesthetized (induction: 5% isofluorance, maintainance 1.5% isofluorane, with room air mixture) and placed in an MRI-compatible cradle equipped to maintain body temperature constant using warm-water circulation. Temperature and respiratory rate were

continuously monitored. T2-weighted anatomical images were first acquired using a RARE-based fast-spin echo sequence with response time = 4,200, echo time = 12, RARE factor 8, 1-mm slice thickness, field of view of 2.4 cm, 256 × 256 pixels, with respiratory gating. Perfusion maps of tumors were then generated using a double spin echo planar pulse sequence using pairs of bipolar gradients at specific predetermined signs in each of three orthogonal directions. The combination of gradient directions allows cancellation of all off-diagonal tensor elements, enabling measurement of the diffusion tensor trace [providing unambiguous and rotationally invariant apparent diffusion coefficient (ADC) values]. Seven b values (b = 0, 50.0, 100, 150, 200, 500, 1,000) were acquired, with a matrix size of 128 × 128, slice thickness 1.0 mm. Volume images (one for each b value) were created from raw DICOM images. For voxels within the 128 × 128 × 15 matrix with a signal value above 2,000, the ADC at each voxel was calculated by using an exponential moving fit by the following method: $ADC = \ln[S(b = b_1) - S(b = b_2)]/(b_2 - b_1)$. The b_1 and b_2 values of 100 and 200, respectively, are sensitive to blood flow apparent diffusion changes in small arteries and capillaries. ADC maps were generated using mono-exponential fitting as above, and T2 images were zero-filled to 256 × 256 before analysis. Parametric images were analyzed in anatomical regions of interest using Bruker Paravision software and offline using Osirix software. All perfusion imaging was performed ≥24 h after the last exercise bout.

Circulating proinflammatory cytokines and metabolic growth factor analysis. ELISA assays were performed using 25 μl of mouse sera in duplicate for each sample with the exception of four samples where sample was only sufficient for a single analysis. Cytokines included VEGF, IFN-γ, IL-1β, IL-10, IL-12p70, IL-6, KC, and TNF-α. Assays were performed on the MSD Sector Imager 2400 (Mesoscale Discovery) using either the Mouse/Rat VEGF Serum/Plasma Kit (Mesoscale K110BMC-1) or the Mouse Pro-Inflammatory 7-plex Ultra-Sensitive Kit (Mesoscale K15012C-1) per manufacturer instructions. Calibration curves using authentic standards of over three orders of magnitude were used to determine analyte concentration in unknowns and lower limit of quantitation/detection. The lower limit of quantification (as determined by coefficient of variation of <20% for standards) for all markers was <10 pg/ml, with the exception of IL-12p70 and IL-6 (lower limit of quantification was 39.1 pg/m). Metabolic growth factors included insulin, insulin-like growth factor 1 (IGF-1) and IGFBP-3 levels evaluated in sera by ELISA (insulin assay, Millipore, Billireca, MA; IGF-1 assay, Diagnostics Systems Laboratory of Beckman Coulter, Webster, TX; IGFBP-3 assay, ALPCO Diagnostics, Salem, NH).

Statistical analysis. Changes in running distance and body weight over time were fitted using fixed-effects linear mixed models. Study outcomes were compared using the Student's t-test for normal distributions, whereas the Wilcoxon Rank-Sums test was used for nonnormal distributions. Analysis of triple replicate prometastatic gene expression used a repeated-measures ANOVA. Circulating proinflammatory cytokines were analyzed in a two-way ANOVA model testing the main effect for treatment while adjusting for day of death. All P values are two sided. Statistical analyses were performed using SAS 9.2 software (SAS Institute, Cary, NC).

RESULTS

Voluntary wheel running exercise behavior and body weight. Median running distance ranged from ~4 to ~6 km/day and significantly decreased across the course of the experiment (P = 0.002; Fig. 1*B*). Body weight increased over the course of the experiment in both groups (P < 0.001; Fig. 1*C*).

Effects of primary tumor growth and metastasis. The primary tumor growth rate was comparable between the exercise and control group across the entire course of the experiment (P > 0.05; Fig. 2*A*). Tumor nodal involvement was 36% lower in the exercise group, but this difference did not reach statistical significance (P = 0.34; data not shown). Similarly, metastatic burden as assessed by the total weight of metastasis

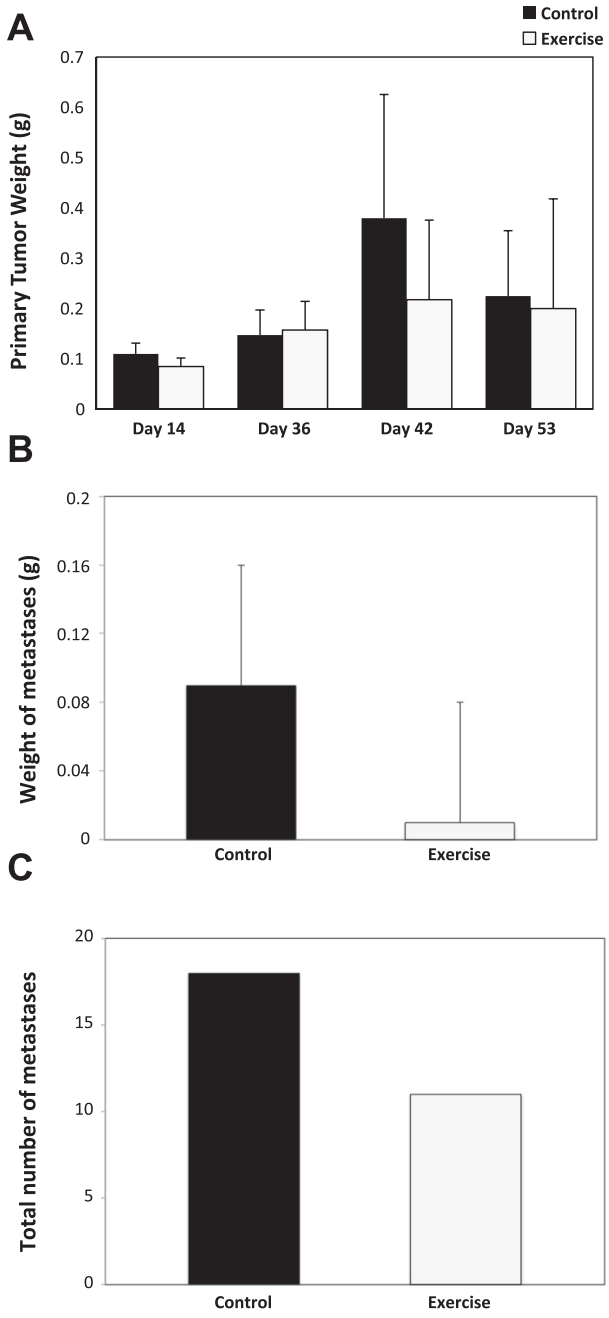

Fig. 2. *A*: primary prostate tumor weight of C57/BL-6 male mice randomized to voluntary wheel running or sedentary control on *day 14* (n = 4/group), *day 36* (n = 4/group), *day 42* (n = 4/group), and *day 53* (n = 18–20/group). Mean primary prostate weights with SE (error bars) are shown. Statistical significance was determined by one-way repeated ANOVA (P > 0.05). *B*: total weight of prostate tumor metastasis of C57/BL-6 male mice randomized to voluntary wheel running or sedentary control (n = 6–8/group across all study timepoints). Total prostate tumor metastasis with SE (error bars) are shown. Statistical significance was determined by an independent samples t-test. *C*: total number of prostate tumor metastasis of C57/BL-6 male mice randomized to voluntary wheel running or sedentary control (across all study time points). Statistical significance was determined by a Wilcoxon Rank-Sums test.

and the total number of metastasis was 88% ($P = 0.18$; Fig. 2*B*) and 34% ($P = 0.25$; Fig. 2*C*) lower, respectively, in the exercise group compared with the control group, but these differences were not statistically significant.

Effects of prometastatic gene expression. Given the lower extent of metastasis in exercising animals, we conducted gene profiling on the primary tumor to examine expression of prometastatic genes (COX2, EGFR, HGFR, CXCR4, MMP2, MMP9, IGF1R). Profiling analysis revealed that CXCR4, an α-chemokine critical for neovascularization and VEGF regulation via its specific ligand stromal-derived-factor-1 (SDF-1 or CXCL12), was approximately twofold higher in the exercise group compared with the control group ($P = 0.002$; Fig. 3*A*). In contrast, hepatocyte growth factor receptor (HGFR) was significantly lower in the exercise group compared with control ($P = 0.003$; Fig. 3*A*). HGFR is regulated via c-Met, which, in turn, elicits multiple cellular responses regulating cell survival, morphogenesis, adhesion, migration, breakdown of extracellular matrix, and angiogenesis. Expression of IGFR-1 and MMP2 were reduced in tumors from exercising mice, but these differences were not significant ($P = 0.10$ and 0.17, respectively; Fig. 3*A*).

Effects on tumor MAPK and PI3K signaling. Tumor cell response to metabolic and angiogenic growth factors is governed by several "core" signaling pathways, most notably extracellular signal-regulated kinases (ERK), mitogen-activated protein kinase (MAPK), and phosphoinositide 3-kinase (PI3K) (4, 25). Western blot analysis revealed that total MEK as well as phosphorylated ERK2-to-total ERK ratio were ~3.5-fold and 2.9-fold higher in the exercising animals relative to sedentary controls with both approaching significance ($P = 0.07$; Fig. 3, *B* and *C*). For PI3K/mTOR signaling, Western blot analysis revealed that both PI3K and mTOR activity was higher in the exercise group, whereas Akt activity was lower, but these differences did not reach significance (data not presented).

Effects on HIF-1, metabolism, and angiogenesis. HIF-1α protein levels were significantly higher in the exercise group relative to control ($P < 0.05$; Fig. 4*A*). The extensive gene expression program regulated by HIF-1 includes genes responsible for cellular metabolism and angiogenesis (27). To gain broad insight, we conducted tumor gene profiling to examine the effects of exercise on expression of a gene set central to these processes. In general, metabolic genes were 2- to 7.5-fold higher in the exercise group; however, only OGDH ($P = 0.03$) reached statistical significance, whereas IDH3α approached significance ($P = 0.06$). Together, these data suggest that exercise increases the expression of metabolic genes in tumors (Fig. 4*B*). In terms of expression of angiogenic genes, levels of the HIF-1 target VEGF were 40% higher in the exercise group relative to control ($P < 0.05$; Fig. 4*C*). Consistent with increased VEGF expression, tumors from exercised animals, in general, also expressed ~1.5- to 6-fold higher levels of angiogenic genes, although only ANGPT2 reached statistical significance ($P = 0.03$) (Fig. 4*D*). Interestingly, FIGF (VEGF-D) ($P = 0.008$) was also significant but with lower levels in tumors from exercising animals.

Effects on tumor perfusion/diffusion and vessel function and maturation. Use of dynamic MR imaging revealed that tumor blood perfusion as well as ADC were significantly higher in exercising animals relative to control ($P < 0.05$; Fig. 5, *A* and

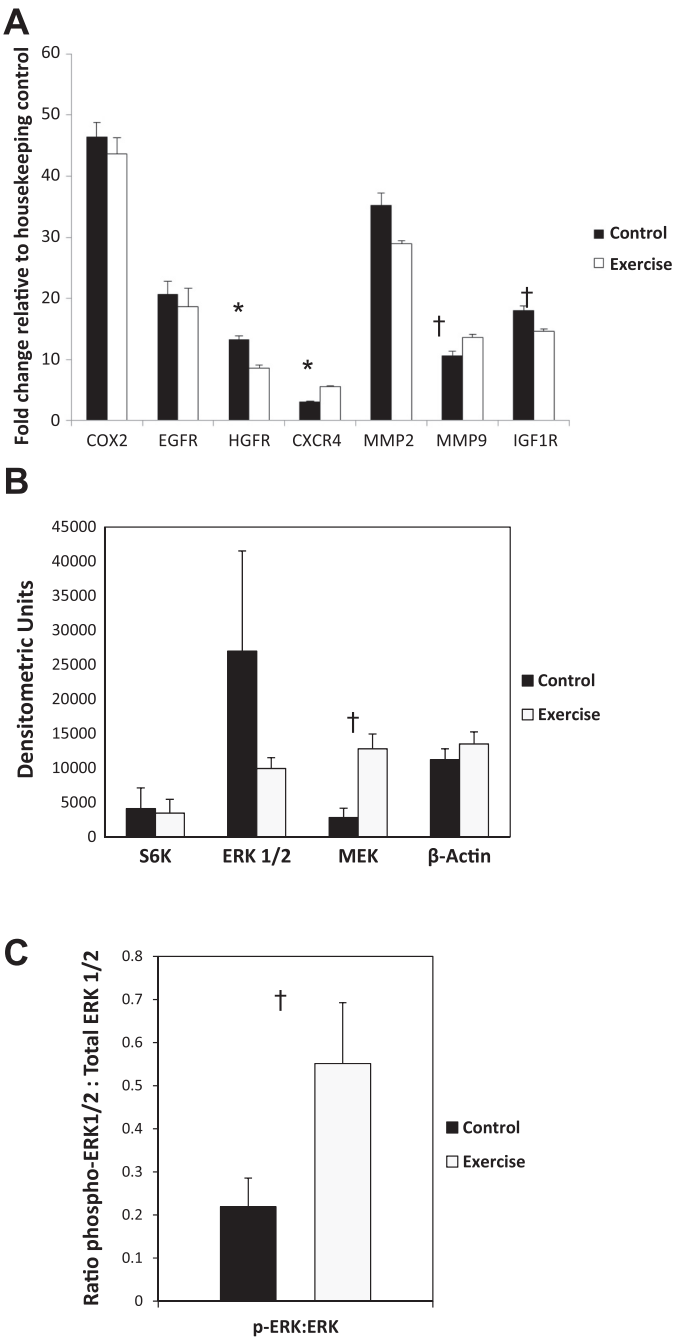

Fig. 3. *A*: expression of prometastatic genes in primary prostate tumors of C57/BL-6 male mice randomized to voluntary wheel running or sedentary control ($n = 6$–10/group). Fold change in exercising animals relative to sedentary control animals are shown. Statistical significance was determined by repeated-measures ANOVA (*$P < 0.05$; †$P < 0.15$). *B*: differences in intratumoral proteins in the extracellular signal-regulated kinases (ERK)/mitogen-activated protein kinase (MAPK) signaling cascade of C57/BL-6 male mice randomized to voluntary wheel running or sedentary control ($n = 6$–10/group). Total densitometric units with SE (error bars) are shown. Statistical significance was determined by a Wilcoxon Rank-Sums test (†$P < 0.15$). *C*: differences in phosphorylated-ERK-to-ERK ratio of C57/BL-6 male mice randomized to voluntary wheel running or sedentary control ($n = 6$–10/group). The ratio of phospho-ERK1/2 to total ERK1/2 with SE (error bars) are shown. Statistical significance was determined by the Wilcoxon Rank-Sums test (†$P < 0.15$).

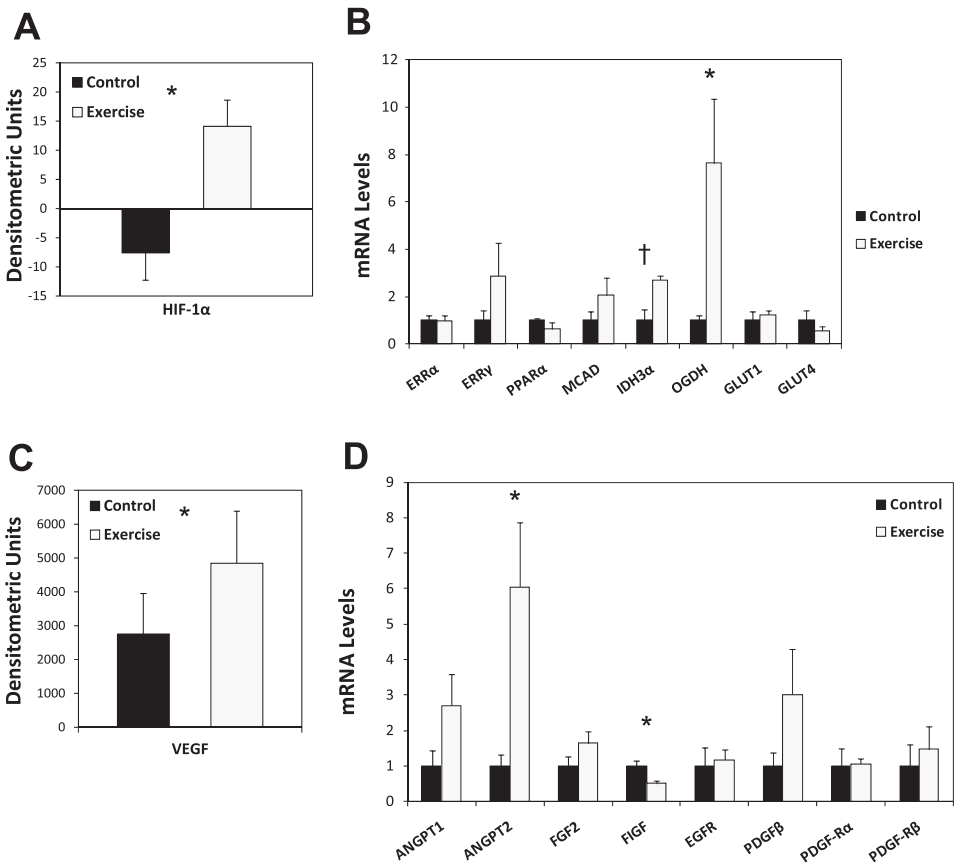

Fig. 4. *A*: levels of hypoxia-inducible factor-1 alpha (HIF-1α) in primary prostate tumors of C57/BL-6 male mice randomized to voluntary wheel running or sedentary control ($n = 6$–10/group). Densitometric units with SE (error bars) are shown. Statistical significance was determined by an independent-samples *t*-test ($^*P < 0.05$). *B*: expression of metabolic genes in primary prostate tumors of C57/BL-6 male mice randomized to voluntary wheel running or sedentary control ($n = 6$–10/group). Total mean mRNA levels in exercising animals relative to sedentary control animals with SE (error bars) are shown. Statistical significance was determined by the Wilcoxon Rank-Sums test ($^*P < 0.05$; $\dagger P < 0.10$). *C*: levels of vascular endothelial growth factor (VEGF) alpha in primary prostate tumors of C57/BL-6 male mice randomized to voluntary wheel running or sedentary control ($n = 6$–10/group). Densitometric units with SE (error bars) are shown. Statistical significance was determined by the Wilcoxon Rank-Sums test ($^*P < 0.05$). *D*: expression of angiogenic genes in primary prostate tumors of C57/BL-6 male mice randomized to voluntary wheel running or sedentary control ($n = 6$–10/group). All data were obtained from animals killed at the end of the study (*day 53*). Total mean mRNA levels in exercising animals relative to sedentary control animals with SE (error bars) are shown. Statistical significance was determined by the Wilcoxon Rank-Sums test ($^*P < 0.05$). ERRα, estrogen-related receptor alpha; ERRγ, estrogen-related receptor gamma; PPARα, peroxisome proliferator-activated receptor alpha; MCAD, medium chain acyl-CoA dehydrogenase; IDH3α, isocitrate dehydrogenase alpha; OGDH, alpha-ketoglutarate dehydrogenase; GLUT1, glucose transporter 1; GLUT4, glucose transporter 4; ANGPT1, angiopoietin 1; ANGPT2, angiopoietin 2; FGF2, fibroblast growth factor 2 (basic); FIGF, c-fos induced growth factor (or vascular endothelial growth factor D); EGFR, epidermal growth factor receptor; PDGFβ, platelet-derived growth factor; PDGF-Rα, platelet-derived growth factor receptor alpha; PDGF-Rβ, platelet-derived growth factor receptor beta.

B). We then investigated how exercise may have caused the observed improvement in blood perfusion. We hypothesized that exercise, via upregulation of angiogenesis, would stimulate vessel branching and endothelial cell maturation leading to improved blood perfusion. mRNA levels of CD31 were ~2.8-fold higher in the exercising animals relative to control animals ($P = 0.014$; Fig. 5*C*), suggesting that exercise increased endothelial vessel density/number.

Effects on circulating proinflammatory cytokines and metabolites. Given exercise-induced modulation of the tumor neoplastic phenotype, we assessed circulating concentrations of cytokines and angiogenic factors [IFN-γ, IL-10, IL-12, IL-1β, IL-6, KC (CXCL1), TNF-α, and VEGF] and metabolic growth (glucose, insulin, IGF-1, IGFBP-1, IGFBP-2, IGFBP-3) axis proteins. Specifically, the proangiogenic factors IL-6 ($P = 0.04$) and KC ($P = 0.03$) were significantly lower in the exercise group relative to the control group (Fig. 6*A*), whereas fasting serum levels of all metabolic growth factors were comparable between groups ($P > 0.05$; Fig. 6*B*).

Skeletal muscle gene profiling. We next exploited gene profiling to investigate whether exercise caused alterations in expression of gene sets responsible for angiogenesis and metabolism in the mid-thigh of the skeletal muscle. Regarding angiogenesis, profiling analysis revealed that several genes responsible for vessel permeability, cell migration, angiogenesis and morphogenesis (VEGF, FIGF), tissue repair, tumor growth and invasion (FGF), vascular homeostasis (ET-1), and endothelial vessel density (CD-31) were significantly higher in the exercise group compared with the sedentary control group (all $P < 0.05$; Fig. 6*C*), indicating that exercise increased skeletal muscle angiogenesis. For metabolism, genes responsible for mitochondrial biogenesis and oxidative metabolism (PGC-1α), fatty acid oxidation (PPARα, MCAD, Agpat3), and glycolysis (OGDH) were significantly or borderline signifi-

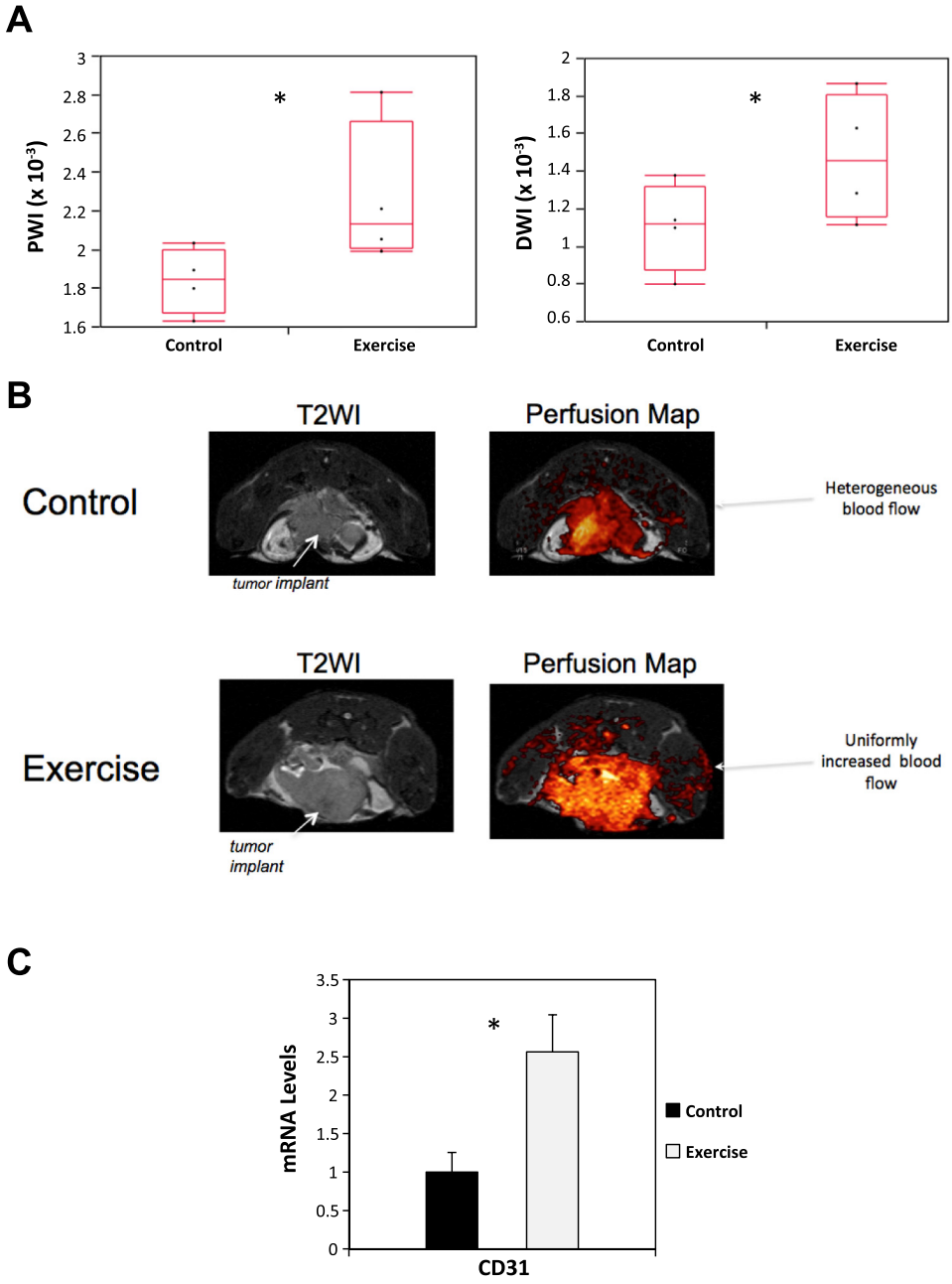

Fig. 5. *A*: intratumoral dynamic MR blood perfusion (*left*) and ADC (*right*) rates in primary prostate tumors of C57/BL-6 male mice randomized to voluntary wheel running or sedentary control (n = 5–6/group). Total weighted image with 95% confidence intervals are shown. Statistical significance was determined by a one-way ANOVA (*P < 0.05). *B*: representative images of increased intratumoral blood perfusion in C57/BL-6 male mice randomized to voluntary wheel running or sedentary control. Tumors from control animals were characterized by heterogenous blood perfusion, whereas tumors from exercising animals were characterized by uniform and increased blood perfusion throughout the tumor microenvironment. *C*: levels of intratumoral CD-31 in primary prostate tumors of C57/BL-6 male mice randomized to voluntary wheel running or sedentary control (n = 6–10/group). All data were obtained from animals killed at the end of the study (*day 53*). Total mRNA levels with SE (error bars) are shown. Statistical significance was determined by the Wilcoxon Rank-Sums test (*P < 0.05).

cantly higher in the exercise group compared with the sedentary control group (all $P < 0.06$; Fig. 6*D*), indicating that exercise augmented skeletal muscle metabolism/energetics in our model.

DISCUSSION

Contrary to our hypothesis, we found that exercise did not inhibit primary cancer progression; however, in partial support, exercise did favorably alter genes responsible for metastatic dissemination in the primary tumor with a shift toward a suppression of distant metastasis in an orthotopic model of murine prostate cancer.

The critical role of HIF-1 activation as a major driver of malignant progression and metastasis is well established (26). As such, given the findings of the present study showing increased HIF-1 and proangiogenic gene expression levels (VEGF, MMP-9, and CXCR4) in tumors from exercising animals, one might expect a shift toward increased as opposed to suppressed metastasis. The precise mechanisms responsible for these contrasting findings are not known but may reflect fundamental differences in the manner of HIF-1 activation. Under normal resting conditions, it is well established that solid tumors have "abnormal" blood vasculature that impairs O_2 delivery and removal of by-products of glycolysis causing hypoxia. Hypoxia stimulates HIF-1 activation that, in turn, induces a robust evasive response including excessive production of proangiogenic pathways (orchestrated by VEGF) in an effort to maintain sufficient O_2 and substrate delivery to support malignancy (27). Paradoxically, this causes nonproductive or pathological angiogenesis, abnormal vessel formation, im-

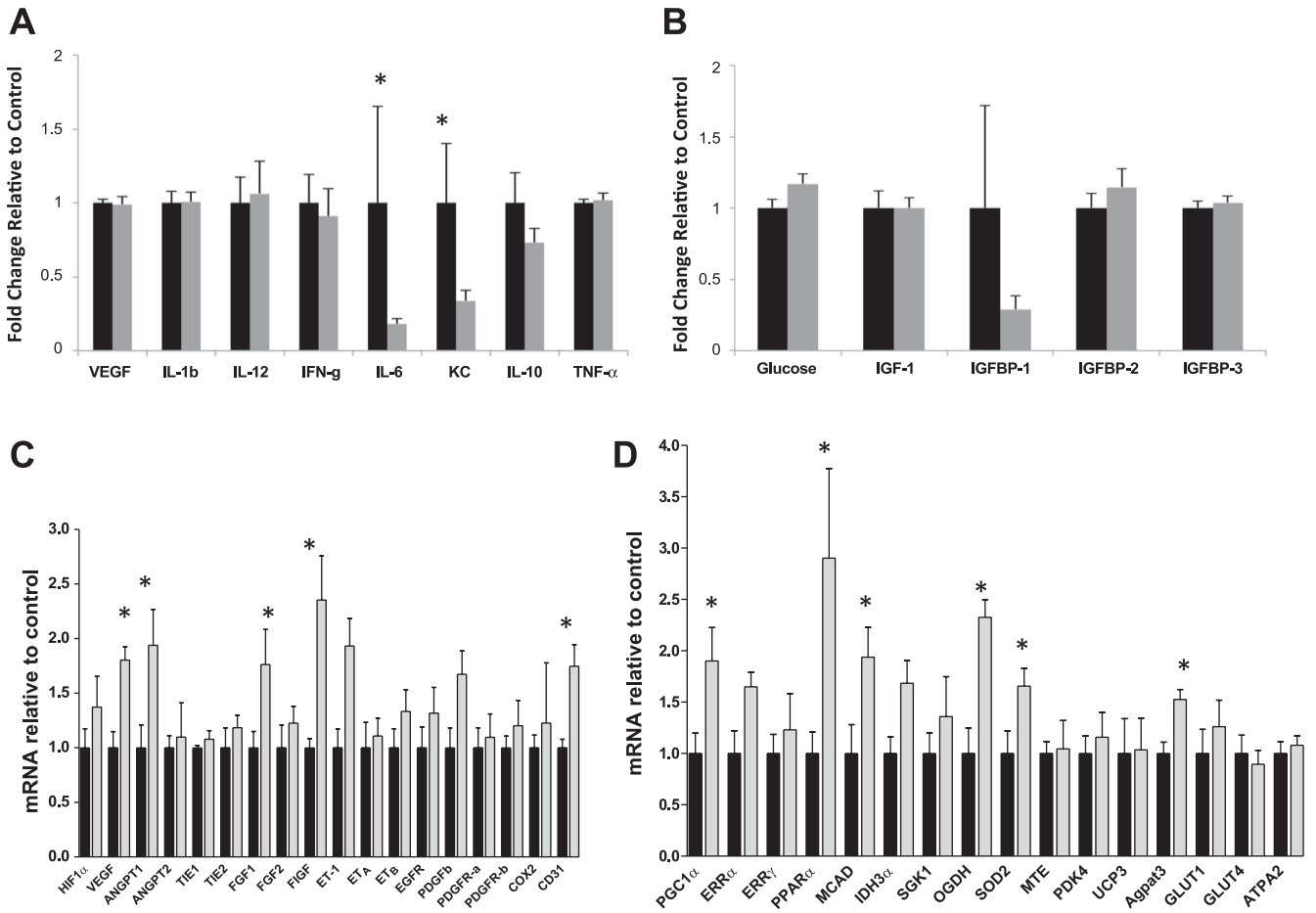

Fig. 6. *A*: plasma levels of proflammatory cytokines and angiogenic factors of C57/BL-6 male mice bearing TRAMP C-1 prostate tumors randomized to voluntary wheel running or sedentary control ($n = 6$–10/group). Fold change in exercising animals relative to sedentary control animals are shown. Statistical significance was determined by testing the treatment effect in a two-way ANOVA (*$P < 0.05$). *B*: plasma levels of metabolic growth factors of C57/BL-6 male mice bearing TRAMP C-1 prostate tumors randomized to voluntary wheel running or sedentary control ($n = 6$–10/group). Fold changes in exercising animals relative to sedentary control animals are shown. *C*: expression of angiogenic genes in skeletal muscle (mid-thigh) of C57/BL-6 male mice randomized to voluntary wheel running or sedentary control ($n = 6$–10/group). Total mRNA levels with SE (error bars) are shown. Statistical significance was determined by the Wilcoxon Rank-Sums test (*$P < 0.06$). *D*: expression of metabolic genes in skeletal muscle (mid-thigh) of C57/BL-6 male mice randomized to voluntary wheel running or sedentary control ($n = 6$–10/group). All data were obtained from animals killed at the end of the study (*day 53*). Total mRNA levels with SE (error bars) are shown. Statistical significance was determined by the Wilcoxon Rank-Sums test (*$P < 0.06$).

paired perfusion/oxygenation, and creation of a self-perpetrating vicious cycle leading to continued hypoxia, increased invasion, and metastasis (3, 19, 22). In stark contrast, we found that exercise-induced stimulation of HIF-1 was associated with an opposite functional outcome: enhanced tumor perfusion/vascularization. This, in turn, was associated with productive or physiological angiogenesis with a resultant shift toward reduced metastasis. This finding extends prior work by our group in which primary tumor growth in female aythmic mice bearing orthotopic human breast carcinomas (MDA-MB-231) was comparable between exercise and control groups, but tumors from exercising animals had significantly higher HIF-1 levels and improved blood perfusion/vascularization (i.e., number of Hoescht perfused vessels) (15). The present findings are, however, in contrast with Zheng et al. (30) and Esser et al. (5), the only other studies to date examining the effects of exercise on prostate tumorgenesis, which found exercise significantly inhibited prostate tumor growth. Differences in cancer type (human vs. mouse), site of implantation (subcutaneous vs. orthotopic), timing of exercise initiation (before establishment of disease), mouse model (immune deficient vs. immune competent vs. transgenic), and amount of exercise likely account for these divergent findings. In terms of the latter, Esser et al. (5) found a dose-response association between exercise and prostate tumorgenesis. Specifically, mice running >5 km/day had significant delays in prostate cancer incidence compared with those running <5 km/day. In similar analyses, we found no significant differences (all $P > 0.05$) in any of the major tumor-related (primary tumor weight, number or weight of metastases) or muscle-related end points in low- vs. high-exercising mice, suggesting the lack of a dose-response association (data not presented). Further work is required to investigate the potential dose-response relationship between exercise and tumor progression/metastasis.

The precise mechanisms underlying exercise-induced stabilization of HIF-1 in solid tumors is not known but may be mediated by both local as well as systemic (host) mechanisms. Regarding local events, exercise is a potent physiological stimulus that profoundly increases mitochondrial demand for O_2/substrate delivery in skeletal muscle and cardiac cells. This

shift in demand (i.e., redistribution of cardiac output) could, in theory, redirect limited O_2/substrate from solid tumors to the exercise-induced metabolically active tissues (e.g., heart, skeletal muscle). We speculate that, in response to exercise-induced perturbations in substrate availability, intratumoral HIF-1 is activated in an effort to maintain local cellular homeostasis (29). Repeated bouts of endurance exercise could therefore stimulate chronic HIF-1 activation leading to increased perfusion and consequently a shift toward a less aggressive phenotype. Regarding systemic (host) mechanisms, in response to acute exercise, skeletal muscle cells secrete several cytokines (known as myokines, including VEGF, TNF-α, IL-6, etc.) into the peripheral circulation that, in a paracrine-like manner, trigger responses in nonmuscle tissues (e.g., the bone marrow) to further augment O_2 and substrate availability/delivery to the skeletal muscle (9). It therefore appears biologically plausible that exercise-induced increases in specific muscle-derived cytokines could enhance ligand binding to their conjugate receptor tyrosine kinase on tumor and/or endothelial cells leading to activation of "core" signaling cascades and stabilization of HIF-1α (as well as other factors). In other words, exercise-induced adaptations in the host may serve to provide highly sought after ligands to tumor cells that effectively "tunes down" the evasive gene program machinery, with a gradual shift toward a less aggressive phenotype. A proangiogenic phenotype also may recruit tumor inhibitory factors to the normoxic tumor microenvironment that, via the production of nitric oxide and accumulation of HIF-1α, enhance immunoregulatory function (28). Indeed, exercise-induced, muscle-derived cytokines inhibit proliferation and increase apoptosis in human breast cancer cells in vitro (10).

The aforementioned described exercise-induced increase in circulating muscle-derived cytokines is, of course, contrary to the findings of this study, which indicated decreased circulating levels of select cytokines following exercise. The opposing effects of acute vs. chronic exercise likely explain these contrasting findings. Specifically, repeated acute bouts of exercise (i.e., chronic exercise) cause global cardiovascular physiological adaptations as well as upregulation of endogenous antioxidant machinery, which together lower circulating levels of proinflammatory cytokines with concomitant increases in anti-inflammatory factors. Consequently, ligand availability in the tumor microenvironment is dramatically altered, leading to inhibition of RTK signaling and decreased tumor aggressiveness/metastatic potential. A gradual alteration in growth factor availability may condition tumor cells to tolerate (as opposed to escape) this microenvironment, thereby preventing a vicious evasive response commonly observed in response to conventional and molecularly targeted cytotoxic therapy (19). In this study, exercise was associated with relatively subtle changes in circulating cytokines; however, given the exquisite sensitivity of tumors, even subtle reductions in host factors may cause dramatic alterations in tumor phenotype and physiology. This creates a new paradigm of how exercise, skeletal muscle physiology, and host-induction and regulation of circulating growth factors may relate to tumor initiation and progression.

In this study, we focused attention on the putative role of circulating cytokines and angiogenic factors integrated with tumor phenotypic markers of hypoxia and angiogenesis to understand the exercise-tumorgenesis relationship. Clearly, however, exercise-induced modulation of additional host-related pathways (e.g., reductions in sex-steroid or metabolic hormone levels, improved immune surveillance, and reduced oxidative damage) in combination with effects on regulators of other classic hallmarks that regulate the neoplastic phenotype (e.g., dysregulated metabolism, sustained proliferative potential, evasion of growth suppressors) (8) could also explain the observed findings. Given the lack of observed changes, it appears that modulation of circulating metabolic growth factors may not have contributed to the observed findings. Similarly, we focused attention on voluntary wheel exercise; thus it is not known whether similar findings would be obtained using forced exercise paradigms such as treadmill running or swimming. Finally, we did not measure food consumption; therefore, we cannot evaluate changes in energy balance with the observed findings. Elucidating the independent vs. additive effects of changes in energy balance via exercise and/or food availability is an important future research goal.

Given the pleiotropic nature of exercise on the host response together with the complexity and diversity of tumor biology, much more mechanistically driven work unraveling the exercise-tumorgenesis relationship is clearly warranted. To this end, our findings suggest future directions for exercise-oncology research. First, the abnormal tumor vasculature and resulting hypoxia poses a formidable barrier to the efficacy of systemic and locoregional anticancer therapies (21), suggesting that exercise via its "normalizing" properties may act as a therapeutic sensitizer. Second, we focused on exercise modulation of the primary tumor phenotype and how such alterations may mediate distant metastasis. In conjunction with such effects, it appears reasonable to speculate that exercise may also inhibit propagation of cells at distant organ sites via modulation of factors influencing dormancy and/or disruption of the "premetastatic" niche (16). Studies of this nature should shed new light on the global mechanistic properties of exercise across different organ systems as well as potential new insights into the biology of metastasis. Finally, use of conventional and molecularly targeted cytotoxic therapy stimulates host-induction of multiple cytokines and angiogenic factors released predominantly to limit or repair normal tissue injury but may inadvertently compromise therapeutic efficacy and accelerate resistance (18). Findings of this study suggest that exercise may be one strategy to neutralize therapy-induced host changes that, in turn, may improve efficacy/delay resistance.

In summary, we report a novel finding of endurance exercise-induced stabilization of HIF-1α with subsequent upregulation of a proangiogenic phenotype stimulating "productive" tumor perfusion (vascularization) with a shift toward reduced metastasis in an orthotopic model of murine prostate cancer. These findings provide new insights into the mechanisms underlying the exercise-cancer progression/metastasis relationship following a cancer diagnosis.

GRANTS

This study was supported in part by research grants from the National Cancer Institute (CA143254, CA142566, CA138634, CA133895, CA125458 to L. W. Jones), Duke Pepper Center, Prostate Cancer Foundation, funds from George and Susan Beischer, and Canadian Institutes for Health Research (J. R. B. Dyck).

DISCLOSURES

No conflicts of interest, financial or otherwise, are declared by the author(s).

AUTHOR CONTRIBUTIONS

Author contributions: L.W.J., J.A., and S.J.F. conception and design of research; L.W.J., J.A., E.M.M., C.D.L., D.F., J.R.D., J.N., C.T.F., A.S.B., E.R.N., M.P., and M.E.Y. performed experiments; L.W.J., E.M.M., G.B., C.D.L., D.F., J.R.D., J.N., C.T.F., A.S.B., E.R.N., M.P., R.C.D., and M.E.Y. analyzed data; L.W.J., M.W.D., R.C.D., and S.J.F. interpreted results of experiments; L.W.J. prepared figures; L.W.J. and J.A. drafted the manuscript; L.W.J., M.W.D., J.R.D., and S.J.F. edited and revised the manuscript; L.W.J., J.A., E.M.M., G.B., C.D.L., D.F., M.W.D., J.R.D., J.N., C.T.F., A.S.B., E.R.N., M.P., R.C.D., M.E.Y., and S.J.F. approved the final version of the manuscript.

REFERENCES

1. **Betof AS, Dewhirst MW, Jones LW.** Effects and potential mechanisms of exercise training on cancer progression: a translational perspective. *Brain Behav Immun*. In press.
2. **DuSell CD, Nelson ER, Wang X, Abdo J, Modder UI, Umetani M, Gesty-Palmer D, Javitt NB, Khosla S, McDonnell DP.** The endogenous selective estrogen receptor modulator 27-hydroxycholesterol is a negative regulator of bone homeostasis. *Endocrinology* 151: 3675–3685, 2010.
3. **Ebos JM, Lee CR, Christensen JG, Mutsaers AJ, Kerbel RS.** Multiple circulating proangiogenic factors induced by sunitinib malate are tumor-independent and correlate with antitumor efficacy. *Proc Natl Acad Sci USA* 104: 17069–17074, 2007.

3a. **Eikelboom R, Mills R.** A microanalysis of wheel running in male and female rats. *Physiol Behav* 43: 625–630, 1988.

4. **Engelman JA.** Targeting PI3K signaling in cancer: opportunities, challenges and limitations. *Nat Rev Cancer* 9: 550–562, 2009.
5. **Esser KA, Harpole CE, Prins GS, Diamond AM.** Physical activity reduces prostate carcinogenesis in a transgenic model. *Prostate* 69: 1372–1377, 2009.
6. **Foster BA, Gingrich JR, Kwon ED, Madias C, Greenberg NM.** Characterization of prostatic epithelial cell lines derived from transgenic adenocarcinoma of the mouse prostate (TRAMP) model. *Cancer Res* 57: 3325–3330, 1997.
7. **Ghosh S, Golbidi S, Werner I, Verchere BC, Laher I.** Selecting exercise regimens and strains to modify obesity and diabetes in rodents: an overview. *Clin Sci (Lond)* 119: 57–74, 2010.
8. **Hanahan D, Weinberg RA.** Hallmarks of cancer: the next generation. *Cell* 144: 646–674, 2011.
9. **Handschin C, Spiegelman BM.** The role of exercise and PGC1alpha in inflammation and chronic disease. *Nature* 454: 463–469, 2008.
10. **Hojman P, Dethlefsen C, Brandt C, Hansen J, Pedersen L, Pedersen BK.** Exercise-induced muscle-derived cytokines inhibit mammary cancer cell growth. *Am J Physiol Endocrinol Metab* 301: E504–E510, 2011.
12. **Jones LW, Liang Y, Pituskin EN, Battaglini CL, Scott JM, Hornsby WE, Haykowsky M.** Effect of exercise training on peak oxygen consumption in patients with cancer: a meta-analysis. *Oncologist* 16: 112–120, 2011.
13. **Jones LW, Peppercorn J.** Exercise research: early promise warrants further investment. *Lancet Oncol* 11: 408–410, 2010.
14. **Jones LW, Viglianti BL, Tashjian JA, Kothadia SM, Keir ST, Freedland SJ, Potter MQ, Moon EJ, Schroeder T, Herndon JE 2nd, Dewhirst MW.** Effect of aerobic exercise on tumor physiology in an animal model of human breast cancer. *J Appl Physiol* 108: 343–348, 2010.
15. **Jones LW, Viglianti BL, Tashjian JA, Kothadia SM, Keir ST, Freedland SJ, Potter MQ, Moon EJ, Schroeder T, Herndon JE 2nd, Dewhirst MW.** Effect of aerobic exercise on tumor physiology in an animal model of human breast cancer. *J Appl Physiol* 108: 343–348, 2010.
16. **Kaplan RN, Riba RD, Zacharoulis S, Bramley AH, Vincent L, Costa C, MacDonald DD, Jin DK, Shido K, Kerns SA, Zhu Z, Hicklin D, Wu Y, Port JL, Altorki N, Port ER, Ruggero D, Shmelkov SV, Jensen KK, Rafii S, Lyden D.** VEGFR1-positive haematopoietic bone marrow progenitors initiate the pre-metastatic niche. *Nature* 438: 820–827, 2005.
17. **Kenfield SA, Stampfer MJ, Giovannucci E, Chan JM.** Physical activity and survival after prostate cancer diagnosis in the health professionals follow-up study. *J Clin Oncol* 29: 726–732, 2011.
18. **Kerbel RS, Ebos JM.** Peering into the aftermath: the inhospitable host? *Nat Med* 16: 1084–1085, 2010.
19. **Loges S, Mazzone M, Hohensinner P, Carmeliet P.** Silencing or fueling metastasis with VEGF inhibitors: antiangiogenesis revisited. *Cancer Cell* 15: 167–170, 2009.
20. **McTiernan A.** Mechanisms linking physical activity with cancer. *Nat Rev Cancer* 8: 205–211, 2008.
21. **Minchinton AI, Tannock IF.** Drug penetration in solid tumours. *Nat Rev Cancer* 6: 583–592, 2006.

21a. **Moraska A, Deak T, Spencer RL, Roth D, Fleshner M.** Treadmill running produces both positive and negative physiological adaptations in Sprague-Dawley rats. *Am J Physiol Regu Integr Comp Physiol* 279: R1321–R1329, 2000.

22. **Paez-Ribes M, Allen E, Hudock J, Takeda T, Okuyama H, Vinals F, Inoue M, Bergers G, Hanahan D, Casanovas O.** Antiangiogenic therapy elicits malignant progression of tumors to increased local invasion and distant metastasis. *Cancer Cell* 15: 220–231, 2009.
23. **Richman EL, Kenfield SA, Stampfer MJ, Paciorek A, Carroll PR, Chan JM.** Physical activity after diagnosis and risk of prostate cancer progression: data from the cancer of the prostate strategic urologic research endeavor. *Cancer Res* 71: 3889–3895, 2011.
24. **Schmitz KH, Courneya KS, Matthews C, Demark-Wahnefried W, Galvao DA, Pinto BM, Irwin ML, Wolin KY, Segal RJ, Lucia A, Schneider CM, von Gruenigen VE, Schwartz AL.** American College of Sports Medicine roundtable on exercise guidelines for cancer survivors. *Med Sci Sports Exerc* 42: 1409–1426, 2010.
25. **Sebolt-Leopold JS, Herrera R.** Targeting the mitogen-activated protein kinase cascade to treat cancer. *Nat Rev Cancer* 4: 937–947, 2004.
26. **Semenza GL.** Targeting HIF-1 for cancer therapy. *Nature Rev Cancer* 3: 721–732, 2003.
27. **Semenza GL.** Targeting HIF-1 for cancer therapy. *Nat Rev Cancer* 3: 721–732, 2003.
28. **Vecchiarelli-Federico LM, Cervi D, Haeri M, Li Y, Nagy A, Ben-David Y.** Vascular endothelial growth factor: a positive and negative regulator of tumor growth. *Cancer Res* 70: 863–867, 2010.
29. **Wagner PD.** Muscle intracellular oxygenation during exercise: optimization for oxygen transport, metabolism, and adaptive change. *Eur J Appl Physiol* 112: 1–8, 2011.
30. **Zheng X, Cui XX, Huang MT, Liu Y, Shih WJ, Lin Y, Lu YP, Wagner GC, Conney AH.** Inhibitory effect of voluntary running wheel exercise on the growth of human pancreatic Panc-1 and prostate PC-3 xenograft tumors in immunodeficient mice. *Oncol Rep* 19: 1583–1588, 2008.